Interaction of Minor Groove Ligands to an AAATT/AATTT Site: Correlation of Thermodynamic Characterization and Solution Structure†

Dionisios Rentzeperis and Luis A. Marky*

Department of Chemistry, New York University, New York, New York 10003

Tammy J. Dwyer, Bernhard H. Geierstanger, Jeffrey G. Pelton, and David. E. Wemmer

Department of Chemistry, University of California, Berkeley, California 94720

Received October 17, 1994; Revised Manuscript Received December 22, 1994®

ABSTRACT: A combination of circular dichroism spectroscopy, titration calorimetry, and optical melting has been used to investigate the association of the minor groove ligands netropsin and distamycin to the central A_3T_2 binding site of the DNA duplex d(CGCAAATTGGC)·d(GCCAATTTGCG). For the complex with netropsin at 20 °C, a ligand/duplex stoichiometry of 1:1 was obtained with $K_b \sim 4.3 \times 10^7$ M^{-1}, $\Delta H_b \sim -7.5$ kcal mol^{-1}, $\Delta S_b \sim 9.3$ cal K^{-1} mol^{-1}, and $\Delta C_p \sim 0$. Previous NMR studies characterized the distamycin complex with A_3T_2 at saturation as a dimeric side-by-side complex. Consistent with this result, we found a ligand/duplex stoichiometry of 2:1. In the current study, the relative thermodynamic contributions of the two distamycin ligands in the formation of this side-by-side complex (2:1 Dst·A_3T_2) were evaluated and compared with the thermodynamic characteristics of netropsin binding. The association of the first distamycin molecule of the 2:1 Dst·A_3T_2 complex yielded the following thermodynamic profile: $K_b \sim 3.1 \times 10^7$ M^{-1}, $\Delta H_b = -12.3$ kcal mol^{-1}, $\Delta S_b = -8$ cal K^{-1} mol^{-1}, and $\Delta C_p = -42$ cal K^{-1} mol^{-1}. The binding of the second distamycin molecule occurs with a lower K_b of $\sim 3.3 \times 10^6$ M^{-1}, a more favorable ΔH_b of -18.8 kcal mol^{-1}, a more unfavorable ΔS_b of -34 cal K^{-1} mol^{-1}, and a higher ΔC_p of -196 cal K^{-1} mol^{-1}. The latter term indicates an ordering of electrostricted and structural water molecules by the complexes. These results correlate well with the NMR titrations and are discussed in context of the solution structure of the 2:1 Dst·A_3T_2 complex.

Distamycin (Dst) and netropsin (Net) (see Figure 1a) belong to a class of DNA binding ligands that show specificity for the minor groove of dA·dT base pairs (Luck et al., 1974; Wartell et al., 1974; Hahn, 1975; Zimmer, 1975; Zimmer & Wähnert, 1986). The molecular basis for the formation of these complexes has been under intensive investigation by a variety of techniques (Taylor et al., 1984; Coll et al., 1987, 1989; Pelton & Wemmer, 1988, 1989, 1990a,b; Rentzeperis et al., 1992, 1993). The binding site for one Dst or Net molecule is four dA·dT base pairs (Pelton & Wemmer, 1988; Kopka et al., 1985). Recent NMR studies, however, indicated that binding sites of at least five base pairs in length can accommodate two Dst molecules side-by-side in an antiparallel orientation (Pelton & Wemmer, 1989, 1990a,b). In this 2:1 complex each ligand preserves all the molecular recognition elements of minor groove binders: electrostatic interactions with the negative potential in the groove of DNA, specific hydrogen bonds of the ligand amide protons with acceptor atoms of the bases, and van der Waals interactions with the wall of the minor groove (Zimmer & Wähnert, 1986; Taylor et al., 1984; Coll et al., 1987, 1989; Pelton & Wemmer, 1988, 1989, 1990a,b; Rentzeperis et al., 1992; Kopka et al., 1985). The side-by-side binding mode has not been observed in the crystal structure of Dst complexed to $d(CGCAAATTTGCG)_2$ (Coll et al., 1989) nor in spectroscopic or calorimetric studies with synthetic DNA homopolymers and heteropolymers containing dA·dT or dI·dC base pairs (Rentzeperis et al., 1992). However, a crystal structure of the side-by-side complex of

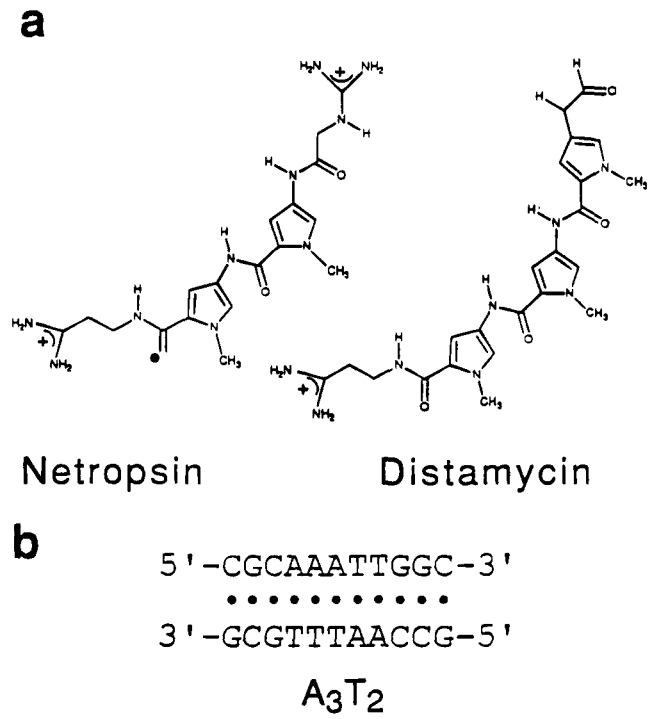

FIGURE 1: (a) Structure of ligands netropsin and distamycin. (b) Sequence of the deoxyoligonucleotide duplex used in these studies.

† Supported by Grants GM-42223 (L.A.M.) and GM-43129 (D.E.W.) from the National Institutes of Health.

* To whom correspondence should be addressed.

® Abstract published in *Advance ACS Abstracts,* February 15, 1995.

0006-2960/95/0434-2937$09.00/0

Dst with $[d(IC)_4]_2$ has been reported (Chen et al., 1994). In contrast to distamycin, the dication netropsin binds only as a single molecule per binding site, suggesting that the side-by-side arrangement of two Net ligands in the minor groove is inhibited by charge interactions. The ease of forming a 2:1 Dst•duplex complex vs a 1:1 Dst•duplex depends highly on the DNA sequence. This cooperativity of 2:1 Dst complex formation has been used to probe sequence-dependent variations in minor groove width (Fagan & Wemmer, 1992; Wemmer et al., 1994). For example, oligomer duplexes containing binding sites with the sequence IIICC/IICCC (Fagan & Wemmer, 1992) or AAGTT/AACTT are occupied only in the 2:1 Dst•duplex mode, and, even at a [Dst]/[duplex] ratio of 0.25:1, no 1:1 complex is observed. Quite the contrary is observed for AAAAA/TTTTT (Fagan & Wemmer, 1992), where 1:1 complexes are observed at low ratios, and 2:1 Dst complex forms only at [Dst]/[duplex] ratios greater than 1:1. These results suggest that while AAAAA/TTTTT exhibits a narrow minor groove favoring the 1:1 Dst binding mode, the wider groove of IIICC/IICCC and AAGTT/AACTT requires the second Dst ligand in the 2:1 complex for tight contacts with the wall of the minor groove [for review, see Wemmer et al. (1994)]. For the central AAATT/AATTT site of d(GCCAAATTGGC)•d(GCCAATTTGCG) (referred to as A_3T_2 duplex hereafter; see Figure 1b), the behavior of Dst binding represents neither of these two extreme cases: up to about a [Dst]/[duplex] ratio of 0.75:1 primarily 1:1 Dst complex is observed, while the 2:1 Dst complex becomes the dominant complex at higher ratios.

In this work, we use a combination of spectroscopic and calorimetric techniques to evaluate the relative thermodynamic contributions of the two Dst ligands to the formation of the dimeric side-by-side Dst complex bound to the central AAATT binding site of the A_3T_2 duplex. The thermodynamic binding profiles are compared to that obtained for the 1:1 complex of Net, and the helix−coil transition of the free A_3T_2 duplex is characterized. Standard thermodynamic binding profiles for the 1:1 binding of Net or the first Dst molecule of the 2:1 Dst•A_3T_2 complex indicate binding affinities in excess of 10^7 M^{-1}. The binding of Net and the first Dst molecule occurs in enthalpy driven processes. However, binding of the second Dst molecule in the 2:1 Dst•A_3T_2 complex takes place with a lower binding affinity of $\sim 10^6$ M^{-1}, consistent with the results from NMR titrations (Pelton & Wemmer, 1989). The large enthalpic contribution to the binding of the second Dst ligand suggests a large increase in van der Waals interactions, probably both between Dst and DNA and between the two Dst molecules, and is partially compensated by an entropic term due to an overall uptake of water molecules. These thermodynamic results of ligand binding are correlated and discussed in terms of the molecular interactions observed in the NMR structure of the Dst•A_3T_2 complexes.

EXPERIMENTAL PROCEDURES

Materials. The complementary strands d(CGCAAATTGGC) and d(GCCAATTTGCG) were synthesized and purified as previously described (Pelton & Wemmer, 1989). The extinction coefficient for each strand was calculated at 25 °C by using the tabulated values of the dimers and monomer bases (Cantor et al., 1970) and was estimated at high temperature by extrapolation to 25 °C of the upper portion of the melting curve. The concentration of the oligomer duplex was determined in aqueous solution using an average extinction coefficient of $\epsilon_{260,90°C} = 103.3$ mM^{-1} cm^{-1} (in single strands). Netropsin-HCl (Net) from Serva Biochemicals and distamycin (Dst) from Sigma were used without further purification. Ligand concentrations were determined in water using $\epsilon_{296,25°C} = 21\,500$ M^{-1} cm^{-1} and $\epsilon_{303,25°C} = 34\,000$ M^{-1} cm^{-1}, for Net and Dst, respectively. All other chemicals were reagent grade. The buffer solution consisted of 10 mM NaP_i and 0.1 mM Na_2EDTA at pH 7.0, adjusted to the desired ionic strength with NaCl. Stock solutions of the oligomer duplex were prepared by dissolving dry and desalted oligomer in the appropiate buffer. Ligand stock solutions in the appropriate buffer were freshly prepared.

Circular Dichroism (CD) Spectroscopy. The CD spectrum of each ligand−DNA complex at several [ligand]/[duplex] ratios was obtained on an Aviv-60DS spectrometer equipped with a thermoelectrically controlled Hewlett Packard cell holder. These spectra allowed definition of the global conformational state of the oligomer duplex and verification of the formation of 1:1 and 2:1 complexes by the presence of isoelliptic points at different [ligand]/[duplex] molar ratios. The stoichiometry of each complex was obtained by following the induced Cotton effect of the bound ligand at ~310 (for Net) and ~333 nm (for Dst) as a function of the [ligand]/[duplex] molar ratio.

UV Melting Curves. Absorbance vs temperature profiles in the appropriate buffer solutions were measured at 260 nm with a thermoelectrically controlled Perkin-Elmer 552 spectrophotometer, interfaced to a PC-XT computer for acquisition and analysis of experimental data. The temperature was scanned at a heating rate of 1.0 °C min^{-1}. Melting curves in buffer solutions were carried out over a 20-fold change in oligomer concentration and at constant strand concentration of ~9 μM over a 10-fold change in salt concentration. From these melting curves, the transition temperature T_m and the van't Hoff enthalpy ΔH_{vH} were obtained using procedures reported previously (Marky & Breslauer, 1987a; Rentzeperis et al., 1991; Zieba et al., 1991). From the slopes of the resulting lines of T_m vs log $[Na^+]$ plots, the release of counterions Δn_{Na^+} (normalized per phosphate) was calculated as reported earlier (Rentzeperis et al., 1991; Zieba et al., 1991).

High Sensitivity Calorimetric Techniques. Excess heat capacity as a function of temperature (DSC melt) was measured with a Microcal MC-2 differential scanning calorimeter (Northampton, MA). Analysis of the resulting curve yielded standard thermodynamic profiles (ΔH_{cal}, ΔS_{cal}, and $\Delta G°_{cal}$) and model-dependent enthalpies ΔH_{vH} of the helix−coil transition of this oligonucleotide duplex. The heats of each ligand interacting with the oligomer duplex were measured directly by titration calorimetry using the Omega calorimeter from Microcal Inc. (Wiseman et al., 1989). Ligand solutions were used to titrate 2 mL (the active volume of the cell is actually 1.4 mL) of oligonucleotide duplex with a 100 μL syringe. Complete mixing was achieved by stirring of the syringe paddle at 400 rpm. The ligand concentration in the syringe was generally at least 30 times higher than any of the oligomer solutions in the reaction cell. The reference cell of the calorimeter was filled with water, and the instrument was calibrated by means of a known standard electrical pulse. Typically, 13 or 21

injections of 6 μL each were performed in a single titration. The area under the resulting peak following each injection is proportional to the heat of interaction Q. When corrected for the titrant dilution heat and normalized to the concentration of added titrant, Q is equal to the binding enthalpy $\Delta H_b'$ at that particular degree of binding. The precision on the heat of each injection is about 1 μcal. Analysis of the calorimetric binding isotherm allowed us to obtain binding affinities and the overall stoichiometry of the complexes in addition to the binding enthalpy. For the 2:1 Dst·A_3T_2 complex, we use a thermodynamic binding model consisting of two sequential and noninteracting sites: the binding of the first Dst ligand to the A_3T_2 site of the free oligonucleotide duplex is characterized by a macroscopic equilibrium constant K_1. The second equilibrium constant, K_2, describes the binding of the second Dst ligand to the same site already filled with one bound ligand. Additionally, an average binding enthalpy ΔH_b and an apparent number of ligands per binding site n (in this case always 1) can be defined for each type of binding site. In general, the calorimetric binding isotherm corresponds to the dependence of the total heat Q_T (or dQ_T/dX_{Tot}) on the total concentration of ligand added (X_{Tot}). The three parameters K_b, ΔH_b, and n for each binding site were determined by interactively fitting the calorimetric binding isotherm using the Marquardt algorithms; the fitting functions used in this procedure, for one or two binding sites, have been described previously (Wiseman et al., 1989; Lin et al., 1991). Initially, all three parameters were free to float. Alternatively, either the enthalpy (which can be obtained independently by averaging the heats of the intermediate peaks of a given site) or n (obtained independently from CD titrations) were fixed, or both, until the lowest standard deviation was obtained.

Determination of Ligand Binding Affinities. Ligand association constants, K_b, were measured from the analysis of the calorimetric binding isotherms as described in the calorimetry section and from the increase in thermal stability of the fully saturated ligand−DNA complexes relative to the free oligomer duplexes. In the latter procedure, the thermal stabilization of the ligand−DNA complex (characterized by ΔT_m) relative to free duplex follows the equation (Crothers, 1970) that was modified to include a variable number of bound ligands for the same site and for the heat of unfolding the number of base pairs that cover just the binding site:

$$\Delta T_m = (T°_m T_m g n R/\Delta H_{hc}) \ln(1 + K_o a_L{}^g) \qquad (1)$$

$T°_m$ and T_m are the transition temperatures of the free and complexed duplexes (with one or two bound ligands), respectively. g is the number of ligands in the complex equal to 1 or 2; n is the apparent number of binding sites per oligomer duplex and is equal to one in all cases. R is the gas constant, while ΔH_{hc} is the dissociation enthalpy of five base pairs (four base-pair stacks) that constitute one binding site, as has been used previously (Rentzeperis et al., 1993; Rentzeperis & Marky, 1993), and is estimated from nearest-neighbor enthalpies (Breslauer et al., 1986). a_L, the activity of the free ligand, is assumed equal to one-half of the total concentration of the ligand at T_m. Equation 1 assumes that binding of either ligand to single-strand DNA is negligible. Ligand binding affinities obtained this way refer to temperatures equal to the transition temperatures of the complexes and are extrapolated to 20 °C by the van't Hoff equation:

$$d \ln K_b/dT = \Delta H_b(T)/RT^2 \qquad (2)$$

where $\Delta H_b(T)$ is the binding enthalpy at temperature T, equal to $\Delta H_b(293) + \int \Delta C_p dT$. In this equation, we used ΔC_p values determined experimentally in this work by calorimetric titrations in the temperature range of 6−20 °C and the integrals are evaluated from $T = T_m$ of the complex to 20 °C.

Table 1: Thermodynamic Profiles for the Formation of the Unligated d(CGCAAATTGGC)/d(GCCAATTTGCG) Duplex at 20°C[a]

T_m (°C)	ΔH_{vH} (kcal/mol)	ΔH_{cal} (kcal/mol)	$\Delta G°_{cal}$ (kcal/mol)	$T\Delta S_{cal}$ (kcal/mol)	d T_m/ d log[Na^+] (°C)	Δn_{Na^+} (mol Na^+/ mol P_i)
55.2	−83	−85.6	−9.2	−76.4	15.7	0.15_4
(69.5)	(−90)	(−82.3)	(−11.9)	(−70.4)		
	−87[b] −86[c]					

[a] The T_ms (±0.5 °C) at the strand concentration of DSC experiments. ΔH_{vH} (±10%) and ΔH_{cal} (±3%) were obtained from the shape and area of the DSC curves, respectively. ΔS_{cal} was calculated form $\int \Delta C_p/T\, dT$ from the DSC curves and $\Delta G°_{cal}$ from the Gibb's equation. The $T\Delta S_{cal}$ values are within ±3%, and the $\Delta G°_{cal}$ values are within ±3% experimental error. Values in paranthesis corresponds to solutions containing 1.0 M NaCl. Spectroscopic transition enthalpies were obtained as follows: [b] ΔH_{vH} from the shape of UV melting curves; [c] ΔH_{vH} from the slope of the plot $1/T_m$ vs ln [C_T/4].

RESULTS

Helix−Coil Transition of the A_3T_2 Duplex

The helix−coil transition of the A_3T_2 duplex was characterized initially by UV melting curves. The transition temperature and the corresponding van't Hoff enthalpy for the uncomplexed A_3T_2 duplex are listed in Table 1. The melting of this duplex occurs in a broad monophasic transition. Characteristic of a bimolecular process, the T_m depends on strand concentration with the van't Hoff transition enthalpy measured to be 87 kcal mol^{-1}. The van't Hoff enthalpy obtained from the $1/T_m$ vs ln [C_T/ 4] plots (Figure 2a) is in excellent agreement with results obtained from the shape of the melting curves. To calculate model-independent transition enthalpies, calorimetric melting curves were measured with a differential scanning calorimeter. A typical excess heat capacity vs temperature profile is presented in Figure 2b. The T_m's, ΔH_{cal}, and ΔH_{vH} values obtained from this curve are also listed in Table 1. The DSC melt is monophasic with no changes in heat capacities within initial and final states. The average ΔH_{cal} of 85.6 and 82.3 kcal mol^{-1} for A_3T_2 determined in 10 mM and 1 M NaCl, respectively, are in good agreement with the enthalpy of 92.6 kcal mol^{-1} estimated from nearest-neighbor parameters in 1 M NaCl (Breslauer et al., 1986). At these two salt concentrations, we obtained an average $\Delta H_{vH}/\Delta H_{cal}$ ratio of 1.03. This duplex, therefore, melts in a two-state transition (Marky & Breslauer, 1987a). Since the model-independent transition enthalpy for this duplex was determined calorimetrically, the overall release of counterions can be calculated from the dependence of T_m on log [Na^+] (Figure 2c). The value of the slope in this plot is 15.7. For the calculation of Δn_{Na^+} per phosphate, all 20 phosphate groups and the average ΔH_{cal} of 84.0 kcal mol^{-1} were taken into

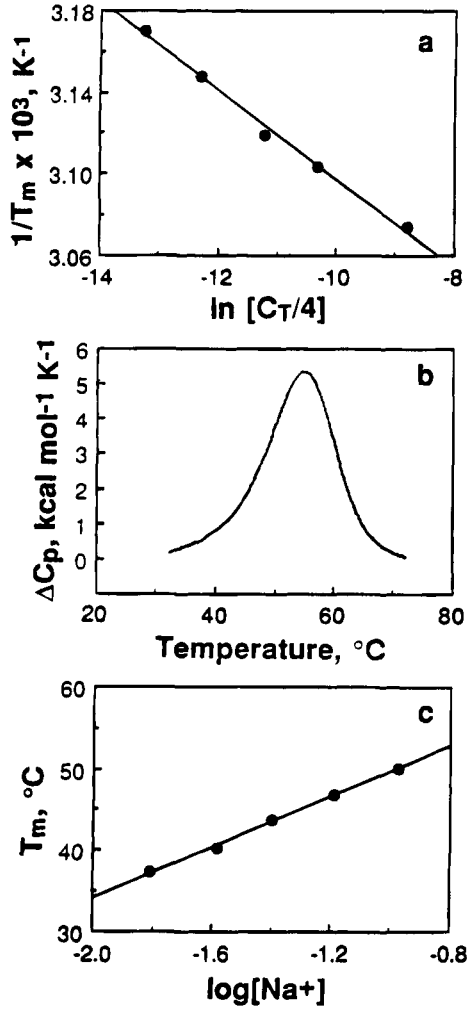

FIGURE 2: Thermodynamic characterization of the helix−coil transition of the d(CGCAAATTGGC)·d(GCCAATTTGCG) duplex in buffer consisting of 10 mM sodium phosphate, 10 mM NaCl, and 0.1 mM Na_2EDTA at pH 7. (a) Dependence of T_m on total strand concentration C_T. (b) Differential scanning calorimetric curve at a total strand concentrations of 0.6 mM. (c) Salt dependence of the T_m.

account. The resulting ion release Δn_{Na^+} of 0.154 Na^+/phosphate is characteristic for oligomer duplexes of this length (Rentzeperis et al., 1993; Zieba et al., 1991; Fenley et al., 1990). Table 1 also lists standard thermodynamic profiles obtained from DSC experiments ($\Delta G°_{cal}$, ΔH_{cal}, and $T\Delta S_{cal}$) for the formation of this duplex at 20 °C. The ΔS_{cal} and $\Delta G°_{cal}$ were calculated with the equations $\Delta S_{cal} = \int(\Delta C_p/T)\, dT$ (evaluated from 10 to 90 °C) and $\Delta G°_{cal} = \Delta H_{cal} - 293.15\Delta S_{cal}$. In the Gibbs equation, both ΔH_{cal} and ΔS_{cal} are assumed independent of temperature and are consistent with the observation of $\Delta C_p = 0$ for this transition. We obtained a favorable $\Delta G°$ term of −13.8 kcal mol^{-1} for duplex formation that results from the partial compensation of a favorable enthalpy with an unfavorable entropy, typical for oligomer duplexes (Rentzeperis et al., 1993a; Zieba et al., 1991).

Interaction of Minor Groove Ligands to the A_3T_2 Duplex

CD Spectra and Stoichiometry of Complexes. A typical CD spectrum for the uncomplexed A_3T_2 duplex, indicative of the B-form DNA conformation, is shown in Figure 3. The addition of Net or Dst results in drastic changes in the

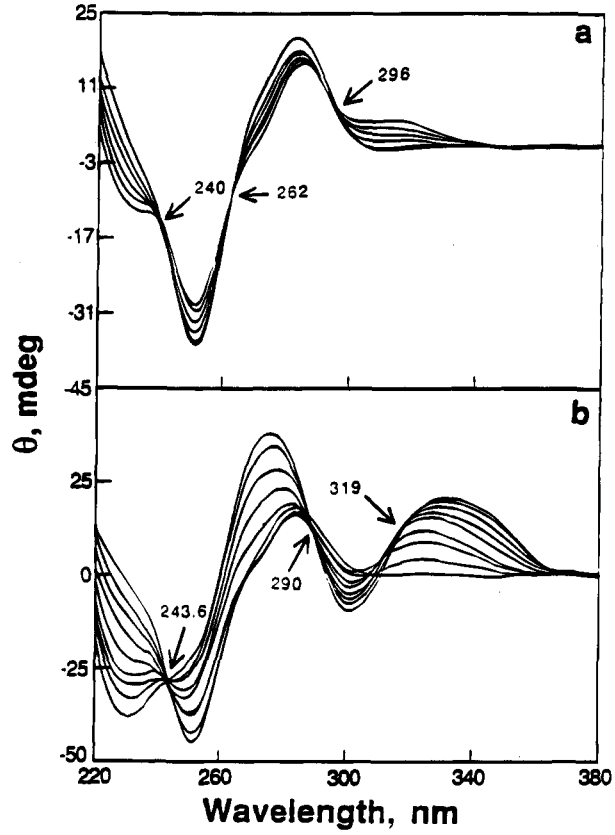

FIGURE 3: Circular dichroism spectra (CD) of the ligand·A_3T_2 complexes at several [ligand]/[duplex] ratios in buffer consisting of 10 mM sodium phosphate, 10 mM NaCl, and 0.1 mM Na_2EDTA at pH 7.0 and 20 °C; (a) with Net and (b) Dst.

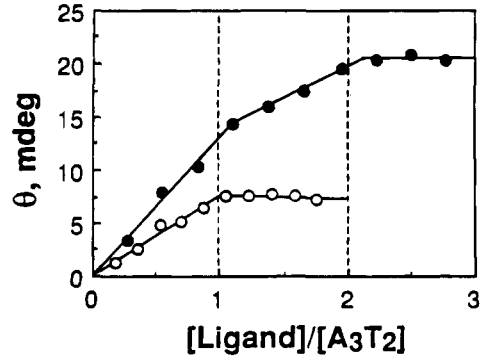

FIGURE 4: CD titrations curves detected at 310 (for Net) and 333 nm (for Dst). Solutions were 10 mM sodium phosphate, 10 mM NaCl buffer, and 0.1 mM Na_2EDTA at pH 7: 2.7 mL of duplex solution in 1 cm quartz cell at a concentration of 5.8 μM duplex titrated with 10 μL aliquots of 0.31 mM Net solution (open circles) or 0.19 mM Dst solution (solid circles).

ellipticity θ except at the well defined isoelliptic points highlighted in Figure 3. In particular, an induced Cotton effect of bound ligand is indicated by the presence of an extra CD band that centers at ~310 nm for Net and ~333 nm for Dst. At these wavelengths, where the optical contribution of DNA is negligible, the changes in ellipticity can be monitored as more ligand is added. The resulting titration curves are shown in Figure 4 for both complexes. Saturation is reached at stoichiometries of 1:1 (ligand molecules per duplex) for the Net·A_3T_2 complex, and 2:1 for the Dst·A_3T_2 complex.

Melting Behavior of Ligand−DNA Complexes. Figure 5 panels a and b show typical differential melting curves for

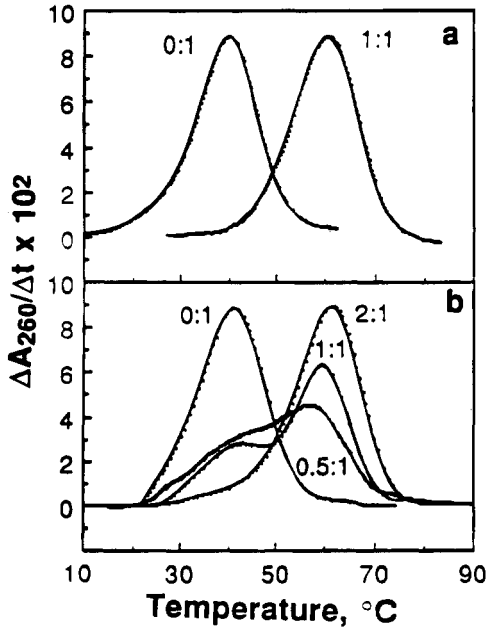

FIGURE 5: Typical differential melting curves of A_3T_2 (at constant duplex DNA concentration of 4.3 μM) in 10 mM sodium phosphate, 10 mM NaCl buffer, and 0.1 mM Na_2EDTA at pH 7.0 at the indicated [ligand]/[duplex] stoichiometries: (a) with Net and (b) with Dst.

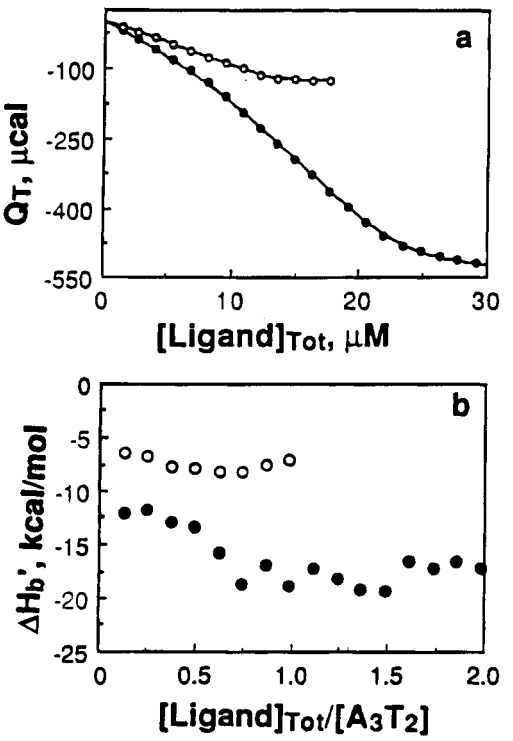

FIGURE 6: (a) Typical calorimetric binding isotherms and the resulting fits (solid lines) in 10 mM sodium phosphate, 10 mM NaCl buffer, and 0.1 mM Na_2EDTA at pH 7.0 and 20 °C: 1.4 mL of duplex solution (11 μM in duplex DNA) titrated with 6 μL aliquots of Net (0.33 mM) (open circles) and Dst (0.32 mM) (closed circles). (b) Dependence of molar binding enthalpies on the degree of ligand binding derived from isothermal calorimetric isotherms (symbols as in panel a). The resulting fitting parameters were identical to those reported in Table 2.

the complexes of the A_3T_2 duplex with Net and Dst, respectively, at several [ligand]/[duplex] ratios. An increase in ligand concentration changes the shape of the melting curves and shifts these curves to higher temperatures. The free duplex and the fully saturated complexes melt in monophasic transitions, while the melting behavior of Dst/A_3T_2 mixtures at [ligand]/[duplex] ratios of 0.5:1 and 1:1 are biphasic. The two T_ms of the biphasic transition at the [ligand]/[duplex] ratio of 1:1 are similar to those of the free and fully complexed duplex. This type of melting behavior is characteristic of ligand–DNA binding processes with K_b values in excess of 10^7 M^{-1} (Rentzeperis & Marky, 1993; Marky et al., 1983). The molar ratios at full saturation correspond approximately to those determined by CD. Most importantly, each fully saturated complex melted with a T_m of 20–21 °C higher than the T_m of the free duplex. Furthermore, the two peaks in the biphasic melting curve of the Dst/A_3T_2 mixtures at a [ligand]/[duplex] ratio of 1:1 have an area ratio of 5 to 8. This suggests the presence of a mixture of complexes with one or two bound Dst molecules, indicating that the value of the binding affinity for the second ligand is similar to that of the first ligand. These observations are consistent with the NMR results reported previously (Pelton & Wemmer, 1989).

Binding of Ligand Results in Exothermic Heats. The heat of each ligand interacting with this oligomer duplex was determined directly by titration calorimetry. The total heat as a function of the total concentration of added ligand for each ligand–duplex system is shown in Figure 6a. In both cases, exothermic heats resulted from ligand binding. These heats level off under saturating conditions corresponding to the stoichiometries obtained in the CD titrations. After a small correction for the heat of dilution of the ligand, the corresponding molar binding enthalpies are calculated as a function of the $[ligand]_{Tot}$/[duplex] ratio (Figure 6b). Binding of Net results in an average ΔH_b of −7.5 kcal mol^{-1} independent of the degree of duplex saturation. For the binding of Dst, $\Delta H_b'$ decreases from −12.5 to −17.5 kcal mol^{-1} at a $[ligand]_{Tot}$/[duplex] ratio of 1 and then remains constant up to the saturation ratio of 2. The latter behavior is consistent with the presence of multiple species in that the overall heat at a given degree of ligand saturation depends on how many duplexes are occupied simultaneously with two Dst ligand molecules or with only one Dst ligand. However, from the fits of the calorimetric titrations we obtained at 20 °C average ΔH_b of −7.5 kcal mol^{-1} for the interaction of Net and ΔH_bs of −12.3 and −18.8 kcal mol^{-1} for the binding of the first and second Dst molecules, respectively (see Table 2). These enthalpy values are independent of both duplex concentration (in the range of 1–11 μM) and salt concentration ranging from 30 to 170 mM NaCl. Therefore, for the association of Dst, the overall magnitude of these enthalpies depends not only on the relative contributions of the molecular interactions observed in the structure of these complexes, i.e., hydrogen bonding and van der Waals contacts, but also slightly on the statistical averaging of the formation heats of all species that are present at a given saturation level. Furthermore, from additional calorimetric titrations at lower temperatures (data not shown), we obtained a ΔC_p of ~0 for the interaction of Net, in agreement with previous results (Marky et al., 1983; Marky & Kupke, 1989), and ΔC_ps of −42 and −196 cal mol^{-1} K^{-1} for the binding of the first and second Dst molecules, respectively.

Binding Affinities and Their Dependence on Salt Concentration. Equation 1 was used to calculate overall ligand binding affinities from UV melting data. These were

Table 2: Binding Enthalpies, Binding Affinities, and Complex Stoichiometries for the Interaction of Ligands with d(CGCAAATTGGC)•d(GCCAATTTCGC)[a]

		From Fits of Calorimetric Isotherms[b]		
ligand	site	ΔH_b (kcal/mol)	K_b (M^{-1})	n (per duplex)
netropsin		-7.5 ± 0.5	4.3 ($\pm$2.1) x 10^7	1.1
distamycin	first	-12.3 ± 0.6	3.1 ($\pm$1.6) x 10^7	1.0
	second	-18.8 ± 0.8	3.3 ($\pm$1.5) x 10^6	1.0

			From UV Melts[c]			
ligand	T°_m (K)	T_m (K)	ΔH_{hc} (kcal/mol)	g (per Duplex)	ΔH_b (kcal/mol)	K_o
netropsin	313.3	333.3	33.2	1	-7.5	4.7 ($\pm$2.3) x 10^7
distamycin	313.5	334.5	33.2	2	-31.1	5.1 ($\pm$2.7) x 10^{14}

[a] Values taken in 10 mM sodium phosphate buffer, 0.1 mM Na_2EDTA, and 10 mM NaCl at pH 7.0 and 20 °C. [b] The concentration of DNA in these titrations was 4.4 μM in duplex. The standard deviation, σ, of the nonlinear fits ranges from 5 to 6% and n within $\pm$0.05. [c] K_o corresponds to the overall binding affinity of the ligands at 20°C.

determined independently from the calorimetric isotherms. The results are listed in Table 2. The overall binding constants at 20 °C and 30 mM NaCl are on the order of $\sim 10^7$ for the association of one Net molecule and $\sim 10^{14}$ for the association of two Dst molecules. The results obtained from these two methods are in general agreement. However, we want to emphasize the fact that the calorimetric measurements are performed near the limit of detection of binding affinities at duplex concentrations of 1−11 μM that are greater than $1/K$. Furthermore, at a stoichiometry near 2:1 the fitting is to the 2:1 binding constant which is closer to 10^6 and hence can be fitted reasonably. In the region near 1:1 stoichiometry what is really being fitted is the difference between the 1:1 and 2:1 binding affinity, this could be done since it is an internal competition of binding modes rather than a bound-free equilibrium. In any case, these K values are best estimates of values greater than 10^6. As indicated by the negative d(ln K_o)/d(ln [Na^+]) values, the magnitude of these binding affinities decreases with increasing salt concentration, a result consistent with the role of electrostatic interactions in the overall formation of these type of complexes (Manning, 1978; Record et al., 1978). The slopes of the ln K_o vs ln [Na^+] plots are -0.80 for the Net•A_3T_2 complex and -0.56 for Dst•A_3T_2 complex.

Thermodynamic Profiles for Ligand Binding. The standard thermodynamic profiles for the interaction of each ligand to the A_3T_2 duplex at 20 °C and 30 mM NaCl are listed in Table 3. The ΔG°_b were derived from the values of K_b according to $\Delta G^\circ_b = -RT \ln K_b$. $T\Delta S_b$ was calculated from the Gibbs equation $\Delta G^\circ = \Delta H^\circ - T\Delta S$. The binding of Net and of the first Dst molecules have K_bs of $\sim 10^7$ M^{-1} ($\Delta G^\circ_b = -10.1$ kcal mol^{-1}) and correspond to enthalpy driven processes, ΔH_bs of -7.5 and -12.3 kcal mol^{-1}, respectively. However, binding of the second Dst molecule takes place with a binding affinity of $\sim 10^6$ M^{-1} ($\Delta G^\circ_b = -8.7$ kcal mol^{-1}) corresponding to a partial enthalpy−entropy compensation process ($\Delta H_b = -18.8$ kcal mol^{-1} and $\Delta S_b = -34$ cal K^{-1} mol^{-1}). The large increase in the exothermicity for the binding of the second Dst ligand, together with the larger heat capacity effect, suggests an increase in van der Waals interactions, which may also be accompanied by the immobilization of water molecules.

DISCUSSION

Solution Structure of the 2:1 Dst•A_3T_2 Complex. The solution structure of the complex of Dst with the A_3T_2 duplex has been determined previously by NMR techniques (Pelton & Wemmer, 1989, 1990). The formation of the 1:1 and 2:1 complexes was monitored by observing new NMR resonances arising from protons on the methylpyrrole rings of the ligand when bound to DNA. At [ligand]/[duplex] ratios of 0.75:1, about 10% of the population of the bound DNA was in the 2:1 complex. At lower ratios than 0.75:1 only 1:1 complexes were detected. It was shown by NOESY experiments at low [ligand]/[duplex] ratios that distamycin binds to 1:1 binding sites on d(CGCAAATTGGC)•d(GCCAATTTGCG). The AAAT/ATTT site is preferred by 2.2:1 over AATT/AATT (Figure 7a). At higher [ligand]/[duplex] ratios, the two Dst ligands bind in the minor groove

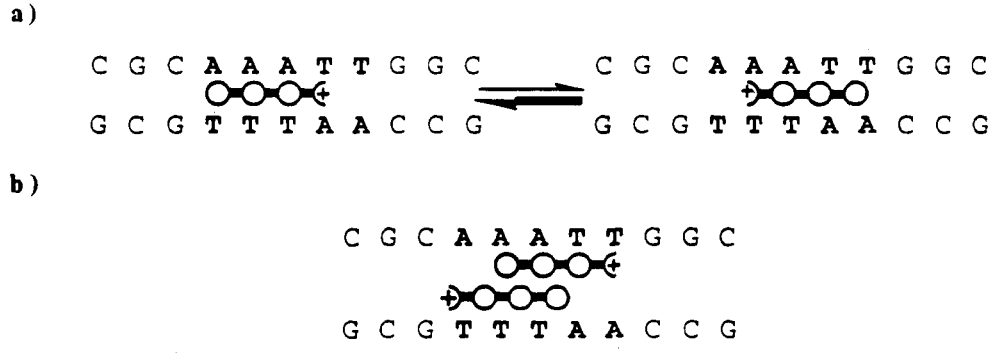

FIGURE 7: Schematic representation of Dst•A_3T_2 complexes as characterized by NMR: (a) 1:1 Dst•A_3T_2 occurring at low [ligand]/[duplex] ratios; (b) 2:1 occurring at [ligand]/[duplex] ratios of about 0.75:1 or higher.

Table 3: Thermodynamic Profiles for the Binding of Minor Groove Ligands to the d(CGCAAATTGGC)•(GCCAATTTGCG) at 20 °C and 30 mM NaCl[a]

ligand	site	ΔG°_b (kcal/mol)	ΔH_b (kcal/mol)	$T\Delta S_b$ (kcal/mol)	ΔC_p (cal/mol-K)	d(ln K_b)/d(ln [Na^+])
netropsin		10.2	-7.5	+2.7		-0.80[b]
distamycin	first	-10.1	-12.3	-2.2	-42	-0.56[b]
	second	-8.7	-18.8	-10.1	-196	

[a] Values were determined from isothermal titration calorimetry (ITC) experiments. Experimental conditions are as in Table 2. The ΔH_b and ΔG° values are within $\pm$5%, and the $T\Delta S_b$ values are within $\pm$8% experimental error. [b] Corresponds to the salt dependence of the overall binding affinity for the interaction of the ligands from UV melting curves.

Table 4: Minor Groove Binding to DNA Duplexes Containing dA·dT Sites

	netropsin			distamycin		
	$K_b(M^{-1})$	ΔH_b (kcal/mol)	d(ln K_b)/d(ln [Na^+])	K_b (M^{-1})	ΔH_b (kcal/mol)	d(ln K_b)/d(ln [Na^+])
			Polymer Duplexes[a]			
d(AT)·d(AT)	5.8×10^9	−12.2	−1.64	3.5×10^9	−19.1	−0.79
d(A)·d(T)	1.5×10^9	−0.4	−1.81	2.7×10^8	−4.0	−0.97
			Oligomer Duplexes			
$[d(GCGAATTCGC)]_2$[b]	2.7×10^8	−9.3	−1.00	2.7×10^8	−15.8	−0.55
d(CCATTAGG)/d(CCTAATGG)[c]	2.6×10^8	−10.6	−1.10			
d(GGATTACC)/d(GGTAATCC)[c]	2.8×10^8	−10.6	−1.10			

Values were taken from the following references: [a] netropsin (Marky & Kupke, 1989), distamycin (Rentzeperis et al., 1992); [b] netropsin at 25 °C (Marky, 1986), distamycin at 25 °C (Breslauer et al., 1987), and unpublished results (Marky). [c] Rentzeperis et al. (1993a) at 5 °C.

of the AAATT/AATTT site, side-by-side with their propylamidinium groups pointing in opposite directions (Figure 7b). Previous studies of 1:1 distamycin complexes with DNA have shown the presence of hydrogen bonds formed between the amide protons of the ligands and the N3 and O2 groups of adenine and thymine groups, respectively (Coll et al., 1989). Molecular modeling of the 2:1 complex, using NMR derived ligand−DNA restraints (Pelton & Wemmer, 1989), indicate that the methylpyrrole rings of one ligand are stacked on top of the amide linkages of the opposite ligand, with the sugar O1′ atoms on the other side. Furthermore, the minor groove widens significantly in order to accommodate both ligands without distorting the B form conformation of the DNA duplex.

Stoichiometry of Complexes. Net and Dst span about four base pairs in their association with a DNA duplex (Zimmer, 1975; Marky et al., 1985). Theoretically, the A_3T_2 undecamer duplex can, therefore, bind up to three ligands: The first ligand with high affinity for the central site of five A·T base pairs and two others with much lower affinity to the G·C base pairs at the ends. The measured stoichiometries of 1:1 for the Net·A_3T_2 and 2:1 for the Dst·A_3T_2 complexes, determined from three different observables (i.e., CD, calorimetric titrations and melting curves of the complexes), together with the magnitude of K_b and ΔH_b, strongly suggest that the binding observed in these studies is only to the five A·T base pairs at the duplex center. However, earlier thermodynamic binding studies of these ligands to synthetic dA·dT polymers and oligomers with a central core of four dA·dT base pairs (Marky et al., 1983, 1985; Marky & Kupke, 1989; Marky, 1986; Breslauer et al., 1986, 1987; Marky & Breslauer, 1987b) showed the binding of only one ligand per site of four or five base pairs. This differential binding behavior of Dst may be due to the actual sequence of the A·T site. Recent NMR results have shown that the cooperativity of the 2:1 Dst binding (i.e., preference for 2:1 complexes) is highly sequence-dependent (Wemmer et al., 1994). While Dst binds exclusively 2:1 to AAGTT/AACTT and ATATA/TATAT even at low [ligand]/[duplex] ratios, only 1:1 Dst complexes are observed with AAAAA/TTTTT at [ligand]/[duplex] ratios up to 1:1. At higher ratios 2:1 Dst complexes form with AAAAA/TTTTT also (Wemmer et al., 1994). The A_3T_2 site is intermediate in its cooperativity for Dst binding. These data suggest that the binding mode of Dst is determined by both sequence-dependent groove width and flexibility.

The First Dst Ligand Binds Like Net with Similar Binding Affinities. At the ionic strength of these studies, the magnitude of K_b for the association of just one Dst ligand is characteristic of the binding of Net and Dst to sites containing all dA·dT base pairs (Marky et al., 1983, 1985; Marky & Kupke, 1989; Marky, 1986; Breslauer et al., 1986, 1987; Marky & Breslauer, 1987b). On the basis of the available structures of Net− and Dst−DNA complexes with different sequences (Pelton & Wemmer, 1988, 1989, 1990a,b; Geirstanger et al., 1993; Patel & Canuel, 1977; Patel, 1979, 1982), we suggest that hydrogen bonding contributions to the overall binding strength are similar. Net and the first Dst molecule of the 2:1 complex have similar overall binding constants. This indicates that the loss of favorable electrostatic interactions in the binding of Dst due to the substitution of one of the charges in Net is compensated by an increase in van der Waals interactions by the extra methylpyrrole rings. The binding of Net ligand and the first Dst ligand in the 2:1 complex is accompanied by exothermic enthalpies. The actual magnitude depends upon the relative contributions of specific hydrogen bonding, van der Waals interactions, and overall hydration of the unligated duplex and of the free ligands. In comparison of these ΔH_bs with those of other sites in oligonucleotides such as AATT and ATTA (see Table 4), our enthalpic values are lower and may be explained in terms of hydration differences due to the increase in the number of AA/TT base-pair stack in the A_3T_2 site as is the case of the differential hydration of dA·dT synthetic oligomers and polymers (Rentzeperis & Marky, 1993; Marky & Kupke, 1989). The entropy contributions are of opposite sign for these ligand, and their overall magnitude and sign depends on the relative contributions from the release of counterions and uptake or release of water molecules.

Increase in van der Waals Interactions between Dst Molecules Results in High Exothermic Enthalpies. Relative to the association of the first Dst ligand in the 2:1 A_3T_2 complex, the second Dst molecule binds with a lower K_b (by a factor of 8) in an enthalpically driven process as seen by the increase of 5.5 kcal mol^{-1} in the exothermicity of the enthalpy. An increase in van der Waals interactions due to the side-by-side contacts between the ligands is the primary reason for this enthalpic term. In addition, if an increase in the hydration state of the complex occurs by electrostriction effects, then the overall amount of bound water will also contribute to the exothermicity of the enthalpy (Rentzeperis et al., 1992; Gasan et al., 1990). Most likely this extra hydration is endothermic (Zieba et al., 1991) because accommodating two ligands in the minor groove leads to a further exposure of organic groups of Dst to solvent that in turn results in a structural rearrangement of water molecules covering the ceiling of the minor groove that is consistent with the observed heat capacity effect. Preliminary volume

change measurements for these association reactions indicate a further uptake of water molecules upon binding of the second Dst molecule (Rentzeperis et al., manuscript in preparation).

Ionic Interactions Differ between Dst and Net. The $[Na^+]$ dependence of K_o (or K_1K_2) shows clearly that binding affinities decrease with increasing salt concentration, as expected since there are clear electrostatic interactions in the stablilization of Dst and Net complexes. The slopes of the ln K_o vs ln $[Na^+]$ plots are -0.80 for the Net·A_3T_2 complex and -0.56 for Dst·A_3T_2 complex. These values are somewhat lower than the -1.00 observed for Net binding to A_2T_2 (Table 4) or -0.55 for one Dst binding to A_2T_2 (Table 4).

These values are also much lower than the theoretical value of -1.76 predicted for the binding of one doubly charged ligand (or two singly charged ligands) from polyelectrolyte theory (Record et al., 1978; Manning, 1978). These differences may be attributed to contributions from several sources: (i) The lower charge density of the ligand free duplex, (ii) hydrophobic contributions due to a different type of dielectric screening by the structural water around the exposed organic groups of the ligand molecules while bound to the minor groove of DNA, and (iii) structural perturbations of the complexes such as the widening of the minor groove upon binding of the second Dst ligand, resulting also in a lower local charge density.

Binding of the Second Dst Molecule Yields a Smaller Release of Counterions. We calculated entropic contributions of +2.7 kcal mol^{-1} and −2.2 kcal mol^{-1} for the association of Net and the first Dst molecule, respectively. However, we observed a further decrease, −10.1 kcal mol^{-1}, for the entropic contribution in the binding of the second Dst molecule. This entropy term is equal to the sum of several contributions: (i) The unfavorable entropy due to a bimolecular association reaction, which is similar for the binding of one ligand; (ii) The release of counterions. In the case of Net, for every mole of bound ligand about 1 mol of sodium ions is released, consistent with previously reported values for oligonucleotide systems (see Table 4). For Dst, which has only one positive charge, we can estimate that binding of the first Dst molecule will release 0.4 mol of Na^+ per mol of ligand (one-half of the Net value, conservative with respect to the value of 0.5 for Dst binding to A_2T_2; Table 4). The overall release from the binding of two Dst molecules is 0.5 mol of sodium ions, suggesting that inclusion of the second ligand results in a release of counterions equal to 0.1 mol per mol of ligand; (iii) The uptake of water molecules which results from the balance of several contributions, including the release of the "spine of hydration" from the minor groove and from the free ligand prior to binding, as well as the uptake of water from the ordering of electrostricted and structural water molecules of exposing polar and nonpolar organic groups to solvent may also contribute.

CONCLUSIONS

The thermodynamic characterization of the A_3T_2 containing oligomer gave values for enthalpy and entropy of duplex formation in line with values determined for many other sequences. The binding of netropsin to this sequence occurs with favorable enthalpy and small, but also favorable, entropy. The values determined are again in agreement with what has been observed for other oligomer sequences. When distamycin is bound to this sequence, the contributions of the first and second molecules can be resolved and their thermodynamic characteristics distinguished. The profile for the first distamycin binding yielded similar affinities and more favorable enthalpy contribution to that of the binding of netropsin. However, the second molecule binding gives a much more favorable enthalpy, interpreted as arising from increased van der Waals interactions, a heat capacity effect, and much less favorable entropy, arising from a combination of ion and water interactions. These contributions lead to a favorable free energy of binding slightly less than that for the first distamycin molecule. The overall ionic strength dependence of binding for the two distamycin ligands suggests that there is a lower counterion release upon binding of the second Dst molecule. The basis for this ion release is unclear at the present time.

These studies reinforce the importance of van der Waals interactions for formation of the 2:1 complex. Understanding the interactions leading to tight binding is valuable input to aid in the development of new sequence-specific ligands, optimized for binding in specific modes to specific sequence targets.

REFERENCES

Breslauer, K. J., Frank, R., Blöcker, H., & Marky, L. A. (1986) *Proc. Natl. Acad. Sci. U.S.A. 83*, 3746−3750.

Breslauer, K. J., Remeta, D. P., Chou, W.-Y., Ferrante, R., Curry, J., Zaunczkowski, D., Snyder, J. G., & Marky, L. A. (1987) *Proc. Natl. Acad. Sci. U.S.A. 84*, 8922−8926.

Breslauer, K. J., Ferrante, R., Marky, L. A., Dervan, P. B., & Youngquist, R. S. (1988) in *Structure & Expression Volume 2: DNA and Its Drug Complexes* (Sarma, R. H., & Sarma, M. H., Eds) pp 273−290, Adenine Press, New York.

Cantor, C. R., Warshow, M. M., & Shapiro, H. (1970) *Biopolymers 9*, 1059−1077.

Chen, X., Ramakrishnan, B., Rao, S. T., & Sundaralingan, M. (1994) *Nature Struct. Biol. 1*, 169−174.

Coll, M., Frederick, C. A., Wang, A. H.-J., & Rich, A. (1987) *Proc. Natl. Acad. Sci. U.S.A. 84*, 8385−8389.

Coll, M., Aymani, J., van der Marel, G. A., van Boom, J. H., Rich, A., & Wang, A. H. (1989) *Biochemistry 28*, 310−320.

Crothers, D. M. (1971) *Biopolymers 10*, 2147−2160.

Fagan, P. A., & Wemmer, D. E. (1992) *J. Am. Chem. Soc. 114*, 1080−1081.

Fenley, M. O., Manning, G. S., & Olson, W. K. (1990) *Biopolymers 30*, 1191−1203.

Gasan, G. I., Maleev, V. Ya., & Semenov, M. A. (1990) *Stud. Biophys. 136*, 171−178.

Geierstanger, B. H., Dwyer, T. J., Bathini, Y., Lown, J. W., & Wemmer, D. E. (1993) *J. Am. Chem. Soc. 115*, 4474−4482.

Hahn, F. E. (1975) in *Antibiotics III: Mechanism of Action of Antimicrobial and Antitumor Agents* (Corcoran, J. W., & Hahn, F. E., Eds.) pp 79−100, Springer, New York.

Kopka, M. L., Yoon, C., Goodsell, D., Pjura, P., & Dickerson, R. E. (1985) *Proc. Natl. Acad. Sci. U.S.A. 82*, 1376−1380.

Lin, L.-N., Mason, A. B., Woodworth, R. C., & Brandts, J. F. (1991) *Biochemistry 30*, 11660−11669.

Luck, G., Triebel, H., Waring, M., & Zimmer, C. (1974) *Nucleic Acids Res. 1*, 503-530.

Manning, G. S. (1978) *Q. Rev. Biophys. 11*, 179−246.

Marky, L. A. (1986) *Polym. Prepr. (Am. Chem. Soc., Div. Polym. Chem.) 27*, 417−418.

Marky, L. A., & Breslauer, K. J. (1987a) *Biopolymers 26*, 1601−1620.

Marky, L. A., & Breslauer, K. J. (1987b) *Proc. Natl. Acad. Sci. U.S.A. 84*, 4359−4363.

Marky, L. A., & Kupke, D. W. (1989) *Biochemistry 28*, 9982−9988.

Marky, L. A., Blumenfeld, K. S., & Breslauer, K. J. (1983) *Nucleic Acids Res. 11*, 2857−2870.
Marky, L. A., Curry, J., & Breslauer, K. J. (1985) in *Molecular Basis of Cancer, Part B: Macromolecular Recognition, Chemotherapy and Immunology* (Rein, R., Ed.) pp 155−173, Alan R. Liss, Inc., New York.
Patel, D. J. (1979) *Eur. J. Biochem. 99*, 369−378.
Patel, D. J. (1982) *Proc. Natl. Acad. Sci. U.S.A. 79*, 6424−6428.
Patel, D. J., & Canuel, L. L. (1977) *Proc. Natl. Acad. Sci. U.S.A. 74*, 5207−5211.
Pelton, J. G., & Wemmer, D. E. (1988) *Biochemistry 27*, 8088−8096.
Pelton, J. G.; & Wemmer, D. E. (1989) *Proc. Natl. Acad. Sci. U.S.A. 86*, 5723−5727.
Pelton, J. G., & Wemmer, D. E. (1990a) *J. Am. Chem. Soc. 112*, 1393−1399.
Pelton, J. G., & Wemmer, D. E. (1990b) *J. Biomol. Struct. & Dyn. 8*, 81−97.
Record, T. M., Jr., Anderson, C. F., & Lohman, T. M. (1978) *Q. Rev. Biophys. 11*, 103−178.
Rentzeperis, D., & Marky, L. A. (1993) *J. Am. Chem. Soc. 115*, 1645−1650.
Rentzeperis, D., Kharakoz, D. P., & Marky, L. A. (1991) *Biochemistry 30*, 6276−6283.
Rentzeperis, D., Kupke, D. W., & Marky, L. A. (1992) *Biopolymers 32*, 1065−1075.
Rentzeperis, D., Ho, J., & Marky, L. A. (1993) *Biochemistry 32*, 2564−2572.
Taylor, J. S., Schultz, P. G., & Dervan, P. B. (1984) *Tetrahedron 40*, 457−465.
Wartell, R. M., Larson, J. E., & Wells, R. D. (1974) *J. Biol. Chem. 249*, 6719−6732.
Wemmer, D. E., Geierstanger, B. H., Fagan, P. A., Dwyer, T. J., Jacobsen, J. P., Pelton, J. G., Ball, G. E., Leheny, A. R., Chang, W.-H., Bathini, Y., Lown, J. W., Rentzeperis, D., Marky, L. A., Singh, S., & Kollman, P. (1994) in *Structural Biology: The State of the Art. Vol 2. Proceedings of the 8th Conversation in the Discipline Biomolecular Stereodynamics* (Sarma, H., & Sarma, M. H., Eds) pp 301−323, Adenine Press, New York.
Wiseman, T., Williston, S., Brandts, J. F., & Lin, L.-N. (1989) *Anal. Biochem. 179*, 131−137.
Zieba, K., Chu, T. M., Kupke, D. W., & Marky, L. A. (1991) *Biochemistry 30*, 8018−8026.
Zimmer, C. (1975) *Prog. Biophys. Mol. Biol. 15*, 285−318.
Zimmer, C., & Wähnert, U. (1986) *Prog. Biophys. Mol. Biol. 47*, 31−112.

BI942426U